Polyhedron 29 (2010) 920–924

Contents lists available at ScienceDirect

Polyhedron

journal homepage: www.elsevier.com/locate/poly

One-dimensional silver(I) 5,5-diethylbarbiturato coordination polymers with *N*-piperidineethanol and 1,3-bis(4-piperidyl)propane: Syntheses, crystal structures, spectroscopic and thermal properties

Veysel T. Yilmaz [a,*], Eda Soyer [a], Orhan Büyükgüngör [b]

[a] Department of Chemistry, Faculty of Arts and Sciences, Uludag University, 16059 Bursa, Turkey
[b] Department of Physics, Faculty of Arts and Sciences, Ondokuz Mayis University, 55139 Samsun, Turkey

ARTICLE INFO

Article history:
Received 1 October 2009
Accepted 29 October 2009
Available online 3 November 2009

Keywords:
5,5-Diethylbarbiturate
N-Piperidineethanol
1,3-Bis(4-piperidyl)propane
Coordination polymers
Silver(I)

ABSTRACT

Two new coordination polymers, $[Ag_2(barb)(pipet)]_n$ (**1**) and $\{Na_3[Ag_2(barb)_2](pippr)\cdot 2H_2O\}_n$ (**2**) (where H_2barb, pipet and Hpippr are 5,5-diethylbarbituric acid, *N*-piperidineethanol and 1,3-bis(4-piperidyl)propane, respectively) have been synthesized and characterized by elemental analysis, IR, thermal analysis and X-ray single-crystal diffraction techniques. Silver(I) ions in complexes **1** and **2** are bridged by barb dianions, leading to one-dimensional coordination polymers. In **1**, the barb ligand acts as a tetradentate bridging ligand, while in **2** as a bidendate bridging ligand. The pipet ligand behaves as a bidentate chelating donor, whereas the pippr anion is not involved in coordination and remains as a counter-ion. The one-dimensional chains of **1** and **2** are further extended into supramolecular networks. Spectral and thermal analysis data for **1** and **2** are in agreement with the crystal structures.

1. Introduction

Barbituric acid is not pharmacologically active and its derivatives possess very interesting pharmaceutical properties and constitute an important group of nervous system depressants and sedative-hypnotics. The coordination chemistry of barbiturates has been developed, due to their use in the detection and identification of these drugs as metal complexes [1,2]. The presence of several potential donor atoms such as two amine nitrogen and three carbonyl oxygen atoms makes barbituric acids polyfunctional ligands. They readily deprotonate in solutions, forming corresponding anions, which usually coordinate in a monodentate fashion through the negatively charged N atoms [3–7], but in some cases, the carbonyl O atoms [8,9] and the C atoms [9,10] are involved in coordination depending on the type of metal ions.

We prepared a number of metal complexes of 5,5-diethylbarbituratic acid ($barbH_2$), also known as barbital or veronal [11–18]. We found that in these complexes, this ligand exist in the form of mono- or dianion, and displays different coordination modes such as monodentate (N), bidentate chelating (N, O), bidentate bridging (N, O) and tridentate bridging (N, O, O). Moreover, simultaneous coordination modes (one barb is N-coordinated and the second barb bidentate or one barb is N-coordinated and the second barb is a counter-ion) are also observed. As part of our continuing interest in the coordination chemistry of 5,5-diethylbarbiturate, in this paper, we report the synthesis and characterization of two coordination polymers of this ligand with other co-ligands, *N*-piperidineethanol (pipet) and 1,3-bis(4-piperidyl)propane (Hpippr), namely $[Ag_2(barb)(pipet)]_n$ (**1**) and $\{Na_3[Ag_2(barb)_2](pippr)\cdot 2H_2O\}_n$ (**2**). Thermal decomposition behavior of complexes **1** and **2** is studied, and their molecular and structural properties were established by single-crystal X-ray diffraction studies.

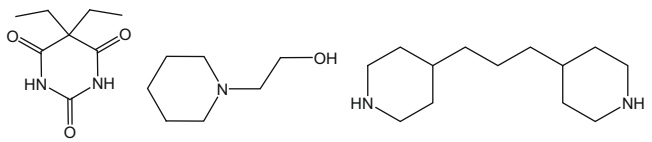

H_2barb pipet Hpippr

2. Experimental

2.1. Materials and measurements

All commercial reagents were purchased and used as supplied. Elemental analyses for C, H, and N were performed using a Costech elemental analyzer. IR spectra were recorded with a Thermo Nicolet 6700 FT-IR spectrophotometer with samples as KBr pellets in

* Corresponding author.
E-mail address: vtyilmaz@uludag.edu.tr (V.T. Yilmaz).

0277-5387/$ - see front matter © 2009 Elsevier Ltd. All rights reserved.
doi:10.1016/j.poly.2009.10.029

the 4000–400 cm^{-1} range. Thermal analysis curves (TGA and DTA) were obtained using a Seiko Exstar 6200 thermal analyzer in a dynamic air atmosphere with a heating rate of 10 °C min^{-1} and a sample size of *ca.* 10 mg.

2.2. Synthesis of the silver(I) complexes

A 10 ml aqueous solution of Na(barbH) (5,5-diethylbarbituric acid sodium salt) (0.21 g, 1 mmol) was added to a 10 ml aqueous solution of $AgNO_3$ (0.17 g, 21 mmol) with stirring at room temperature. The solution immediately became milky. The addition of *N*-piperidineethanol (pipet) (0.13 ml) together with a mixture of 2-propanol (PrOH) and acetonitrile (MeCN) (1:1) (10 mL) to the milky suspension resulted in a clear solution. The resulting solution was allowed to stand in darkness at room temperature and colorless prisms of $Ag_2(barb)(pipet)]_n$ (**1**) were obtained after 3 days. Yield 62%. M.p. 142–145 °C (decomp). *Anal.* Calc. for $C_{15}H_{25}Ag_2N_3O_4$: C, 34.2; H, 4.8; N, 8.0. Found: C, 34.4; H, 4.6; N, 8.2%. IR (cm^{-1}): 3408sb, 3179mb, 3052vw, 2974w, 2934vw, 2876w, 1695s, 1671vs, 1634s, 1585s, 1556vs, 1458sh, 1422vs, 1381vs, 1344m, 1311vs, 1262s, 1181vw, 1033vw, 939w, 854m, 792w, 764w, 694w, 653vw, 551w, 445w.

$\{Na_3[Ag_2(barb)_2](pippr)\cdot 2H_2O\}_n$ (**2**) was synthesized in a similar way, replacing pipet with Hpippr. Yield 65%. M.p. 150 °C (decomp). *Anal.* Calc. for $C_{29}H_{29}Ag_2N_6Na_3O_8$: C, 38.8; H, 5.8; N, 9.4. Found: C, 38.7 H, 5.6; N, 9.5%. IR (cm^{-1}): 3403sb, 3260m, 2966sh, 2917s, 2848s, 1708m, 1671s, 1630s, 1601vs, 1548vs, 1446s, 1418s, 1360s, 1311vs, 1279m, 1181vw, 1156vw, 1103w, 1033w, 952w, 858w, 805w, 756w, 633vw, 613vw, 539vw, 478vw.

2.3. X-ray crystallography

The intensity data of the complexes **1** and **2** were collected using a STOE IPDS 2 diffractometer with graphite-monochromated Mo Kα radiation (λ = 0.71073). The structures were solved by direct methods and refined on F^2 with the SHELX-97 program [19]. All non-hydrogen atoms were found from the difference Fourier map and refined anisotropically. All C hydrogen atoms were included using a riding model. The H atoms of the OH group of pipet in **1** and water molecules in **2** were refined freely. The details of data collection, refinement and crystallographic data are summarized in Table 1.

Table 1
Crystallographic data and structure refinement for **1** and **2**.

	1	**2**
Formula	$C_{15}H_{25}Ag_2N_3O_4$	$C_{29}H_{29}Ag_2N_6Na_3O_8$
Molecular weight	527.12	894.45
Temperature (K)	298(2)	296(2)
Wavelength (Å)	0.71073	0.71073 Å
Crystal system	triclinic	monoclinic
Space group	$P\bar{1}$	$P2_1/c$
Unit cell dimensions		
a (Å)	7.3494(5)	14.4356(12)
b (Å)	11.3548(8)	15.1833(7)
c (Å)	11.3832(7)	22.3716(19)
α (°)	77.624(5)	90
β (°)	76.630(5)	127.298(5)
γ (°)	88.814(6)	90
Volume (Å^3)	902.30(11)	3900.6(6)
Z	2	4
Calculated density (g/cm^3)	1.940	1.523
μ (mm^{-1})	2.194	1.088
F(0 0 0)	524	1824
Crystal size (mm^3)	0.58 × 0.24 × 0.07	0.50 × 0.26 × 0.03
θ Range (°)	2.33–26.50	1.76–27.00
Index ranges (*h*, *k*, *l*)	−9/9; −14/14; −14/14	−17/18; −19/19; −28/28
Reflections collected	12 574	34 104
Independent reflections	3739 [R_{int} = 0.0489]	8518 [R_{int} = 0.1134]
Reflections observed (>2σ)	3475	4539
Absorption correction	numerical	numerical
Data/parameters	3739/223	8518/413
Goodness-of-fit (GOF) on F^2	1.156	0.988
Final *R* indices [$I > 2\sigma(I)$]	R_1 = 0.0294 wR_2 = 0.0705	R_1 = 0.0672 wR_2 = 0.1436
Largest differences in peak and hole (e Å^{-3})	0.611 and −1.102	1.309 and −1.928

3. Results and discussion

3.1. Synthesis and characterization

Complexes **1** and **2** were synthesized by the direct reaction of Na(Hbarb) with $AgNO_3$ in the aqueous solution in the presence of the pipet and Hpippr ligands. They were obtained in moderate yields (over 60%). Both complexes are air stable and soluble in a mixture of water, EtOH and MeCN (1:1:1).

Selected FT-IR spectroscopic data are listed in Table 2. The IR spectra of both complexes display strong and broad absorption bands at around 3400 cm^{-1}, due to the OH group vibrations. The absorption bands of the amine groups appear at 3179 cm^{-1} in **1**, and 3260 cm^{-1} in **2**. Medium and weak bands between 2848 and 3052 cm^{-1} correspond to the CH stretching vibrations. Since the barbH2 ligand contains three carbonyl groups, the coordination of this ligand is easily deduced from the IR spectra. Complexes **1** and **2** present three absorption bands in the frequency range 1610–1708 cm^{-1}, which are indicative of the unequal coordination of the carbonyl groups. The bands below 1600 cm^{-1} are due to the CC stretching, CH deformation and CN stretching vibrations as given in Table 2.

3.2. Crystal structures

A view of the coordination environment around silver(I) in **1** is shown in Fig. 1a, together with the atom numbering scheme. Selected bond distances and angles are listed in Table 3. Single X-ray crystal analysis reveals that the complex crystallizes in triclinic space group $P\bar{1}$ and is a one-dimensional neutral metallopolymer. In **1**, the barb ligands are in the form of dianions, acting as a tetradentate bridging ligand between four silver(I) centers through two negatively charged N and two carbonyl O atoms, forming centrosymmetric tetranuclear units. To the best of our knowledge, the tetradentate coordination mode of the barb dianion was observed for the first time in this complex. The tetranuclear units are linked by the N(barb)–Ag–N(barb) bridges, leading to a linear polymeric chain propagating along the *c* axis (Fig. 1b). The present coordination polymer has three non-equivalent silver(I) ions. The coordination geometry around the Ag1 atom is a highly distorted tetrahedron with an $AgNO_3$ chromophore, whereas Ag2 and Ag3 atoms have distorted linear coordination geometry of AgN_2. The tetranuclear unit exhibits Ag–Ag interactions with a Ag···Ag separation of 2.9283(3) Å, being much smaller than twice the van der

Table 2
Selected FT-IR spectral data[a] for **1** and **2**.

Assignment	**1**	**2**
ν(OH)	3408sb	3403sb
ν(NH)	3179mb	3260m
ν(CH)	3052vw, 2974w, 2934vw, 2876w	2966sh, 2917s, 2848s
ν(CO)	1695s, 1671vs, 1634s	1708m, 1671s, 1630s
ν(CC)	1585s, 1556vs	1601vs, 1548vs
δ(CH)	1422vs, 1381vs, 1344m, 1311vs	1418s, 1360s, 1311vs
ν(CN)	1262s	1279m

b = broad; m = medium; w = weak; vw = very weak; vs = very strong; s = strong.
[a] Frequencies in cm^{-1}.

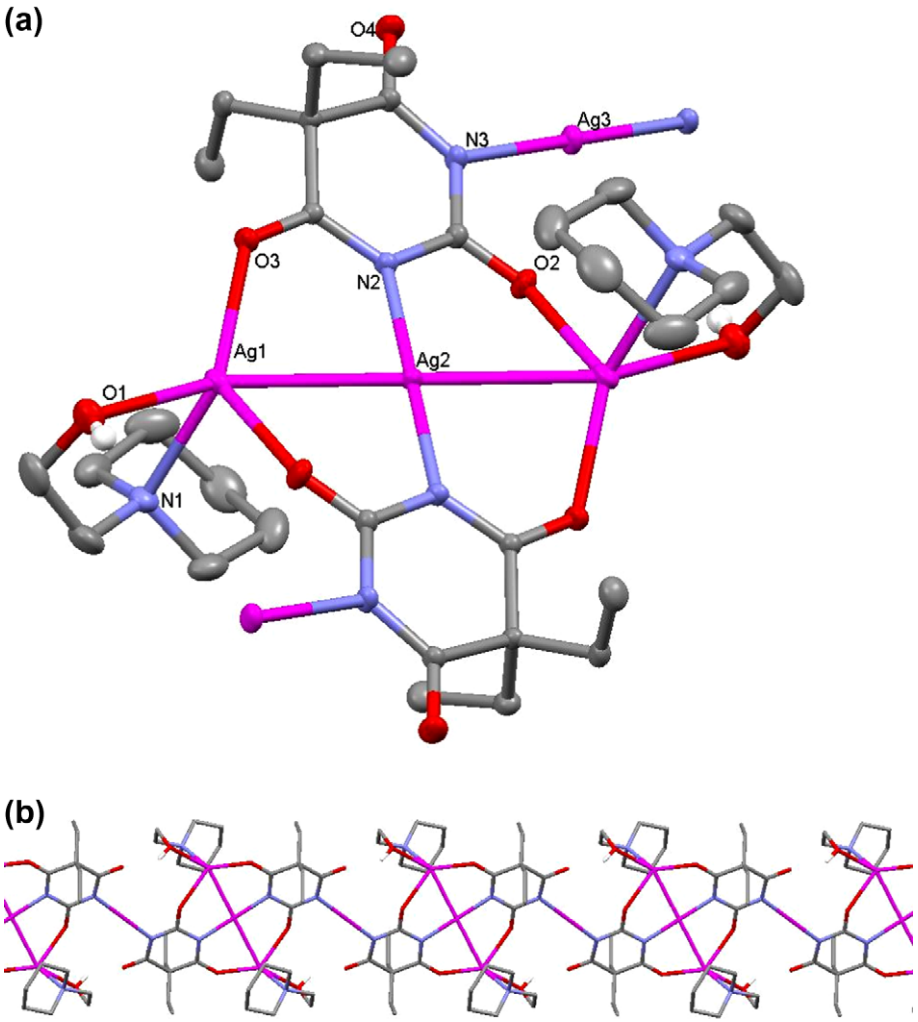

Fig. 1. (a) Coordination environment around silver(I) ions in **1**, (C–H hydrogen atoms were omitted for clarity). (b) A perspective view of the one-dimensional chain in **1**.

Table 3
Selected bond and hydrogen bonding geometry for **1**.

Bonds lengths (Å) and angles (°)				
Ag1–N1	2.321(3)	N1–Ag1–O1		74.92(12)
Ag2–N2	2.085(2)	N1–Ag1–O2		95.15(11)
Ag3–N3	2.090(2)	N1–Ag1–O3		133.69(11)
Ag1–O1	2.546(3)	O1–Ag1–O2		81.99(9)
Ag1–O2	2.459(3)	O1–Ag1–O2		120.74(9)
Ag1–O3	2.262(2)	O2–Ag1–O3		128.36(10)
Ag1–Ag2	2.9283(3)			
Hydrogen bonds				
D–H···A	D–H (Å)	H···A (Å)	D···A (Å)	D–H···A (°)
O1–H1···O4	0.82(6)	2.09(4)	2.835(4)	149(6)

Waals radius of silver (3.44 Å), indicating a strong interaction between the silver(I) ions.

The Ag–N(barb) bond distances are 2.085(2) and 2.090(2) Å are practically similar to those found in $[Ag(barb)(\mu\text{-bpe})]_n$ [12], but somewhat longer than those found $Na_3[Ag_3(\mu\text{-barb})_6]$ [12], $\{[Ag_2(\mu\text{-barb})_2][Ag_2(\mu\text{-en})_2]\cdot 5H_2O\}_n$ [12], while they are significantly shorter than the corresponding distances found in [Ag(barb)(bpy)] [15], [Ag(barb)(pypr)] [15], [Ag(barb)(pym)]·H_2O [18] and [Ag(barb)(dmpy)]·1.5H_2O [18]. Again, the coordination of the barb ligand to silver(I) ion via the carbonyl O atoms was observed for the first time. The Ag–O(barb) bond distances are much longer, compared to Ag–N(barb) bond distances. On the other hand, the pipet ligand is neutral and behaves as a bidentate chelating ligand via the N atom and hydroxyl O atoms. The Ag–N(pipet) and Ag–O(pipet) bond distances are comparable to those found in [Ag(sac)(hepip)] [20].

The pyrimidine ring of the barb ligand is essentially planar and the three carbonyl groups are not significantly displaced from the mean planes of their attached pyrimidine ring, whereas the piperidine moiety of pipet exhibits a chair conformation. A packing diagram of complex **1** is shown in Fig. S1. The individual chains show a two-dimensional array along the *ac* plane.

The asymmetric unit of complex **2** is shown in Fig. 2a and selected bond length and angles are listed in Table 4. Complex **1** consist of a $[Ag_2(barb)_2]^{2-}$, three Na^+ and a deprotonated pippr ions, and two lattice water molecules. As shown in Fig. 2a and b, the complex is a coordination polymer, in which the barb dianions bridge the silver(I) cations giving rise to a one-dimensional zigzag chain. All silver(I) ions are linearly coordinated by both negatively charged N atoms of the barb ions and all Ag–N bond distances are almost identical, being slightly longer than those found in complex **1**. The pippr monoanion is not involved in coordination with silver(I) and remains a counter-ion.

The complex contains three different sodium(I) ions. The barb anions also act as a bridge between two sodium(I) cations (Na1 and Na2) through their carbonyl groups, while the Na3 atom are linearly coordinated by the deprotonated N atom of pippr and

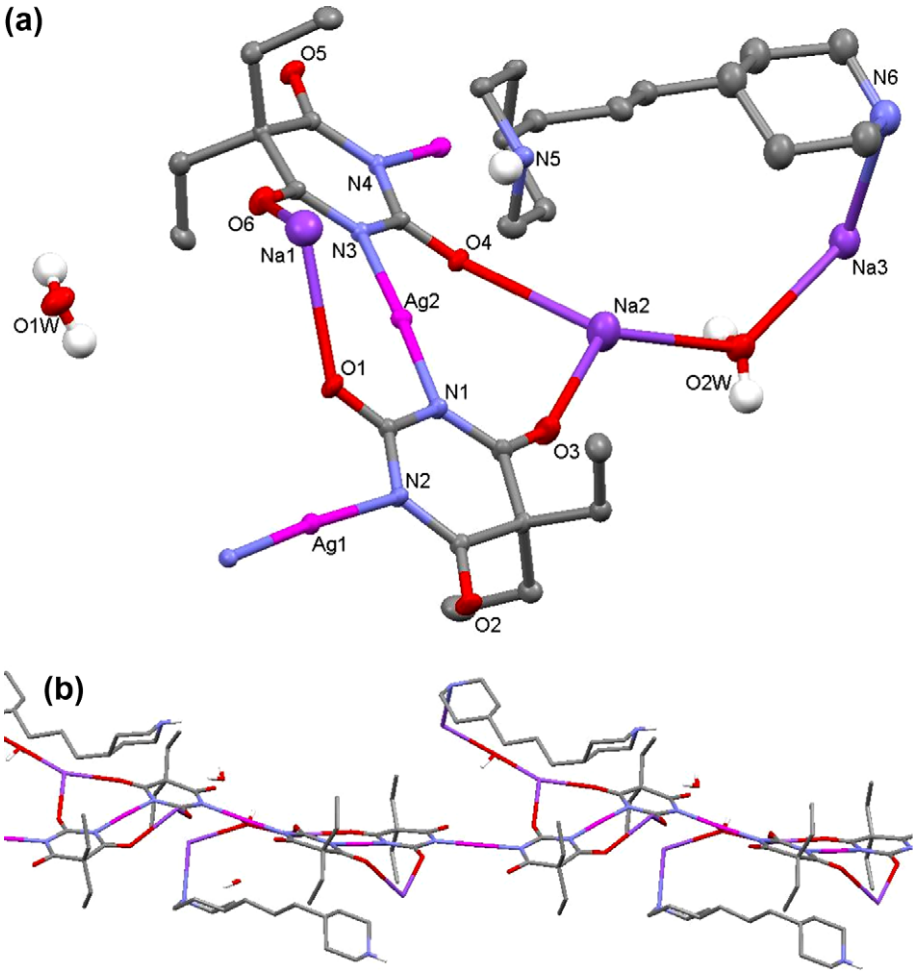

Fig. 2. (a) Coordination environment around silver(I) and sodium(I) ions in **2**, (C–H hydrogen atoms were omitted for clarity). (b) A fragment of the one-dimensional chain in **2**.

Table 4
Selected bond and hydrogen bonding geometry for **2**.

Bonds lengths (Å) and angles (°)				
Ag1–N2	2.110(5)	N2–Ag1–N4^{i}		175.6(2
Ag1–N4^{i}	2.104(5)	N1–Ag1–N3		177.4(2)
Ag2–N1	2.098(6)	N6–Na3–O2W		111.9(3)
Ag2–N3	2.097(6)	O1–Na1–O6		100.0(3)
Na1–O1	2.751(9)	O3–Na2–O4		100.2(3)
Na2–O3	2.764(8)	O3–Na2–O2W		127.7(3)
Na2–O4	2.906(8)	O4–Na2–O2W		126.3(3)
Na1–O6	2.792(9)			
Na2–O2W	2.806(10)			
Na3–O2W	2.903(9)			
Na3–N6	2.719(13)			
Hydrogen bonds[a]				
D–H···A	D–H (Å)	H···A (Å)	D···A (Å)	D–H···A (°)
O1W–H12W–N6	0.82(13)	2.02(9)	2.717(15)	142(12)
N5–H5···O2^{i}	0.86(7)	1.95(8)	2.796(8)	166(8)
O1W–H11W–O2^{ii}	0.83(7)	2.15(11)	2.701(10)	124(12)
O2W–H21W–O5^{iii}	0.83(8)	1.99(6)	2.784(9)	158(13)
O2W–H22W–O1W^{iv}	0.84(9)	2.01(7)	2.760(12)	148(10)

[a] *Symmetry codes:* (i) $x-1, -y+1/2, z-1/2$; (ii) $x, -y+1/2, z-1/2$; (iii) $-x+1, -y+1, -z$; (iv) $-x+2, y+1/2, -z+1/2$.

one of the lattice water O atom, which acts as a bridge between the Na2 and Na3 atoms (Fig. 2a). The Na–O(barb) bond distances range from 2.751(9) to 2.906(8) Å, being significantly longer than those reported for $Na_3[Ag_3(barb)_6]$ [12] and Na(Hbarb) [21].

Both piperidine moieties of pippr show a chair conformation. The barb ligands are essentially planar and the dihedral angle between the mean planes of the pyrimidine rings of two neighboring barb ligands is 15.93(5)°. The polymeric chains run parallel to the *c* axis and are further cross-linked by the OW–H–O(barb) type intermolecular hydrogen bonds, leading to a three-dimensional supramolecular network (Fig. S2).

3.3. Thermal decomposition

Thermal decomposition and stability of both complexes were studied by TGA and DTA at the atmosphere of air in the temperature range 25–900 °C. Thermal curves are illustrated in Fig. 3. Complex **1** is stable up to 145 °C and begins to release the pipet ligand between 145 and 212 °C. The mass loss of 23.7% in this stage is consistent with the calculated value of 24.5%. Then, the highly exothermic decomposition of the barb moiety occurs in the temperature range 215–448 °C to yield the metallic silver. Complex **2** dehydrates between 40 and 106 °C with a mass loss of 5.5% (calcd. 4.0%) and dehydrated complex is stable up to the 149 °C. Then, a 3.2% mass loss was observed between 149 and 185 °C, followed by a continuous mass loss related to decomposition of both pippr and barb ligands in the range of 149–467. The endothermic DTA peak at centered at 210 °C correspond to the elimination of the aepip ligand, while the violently exothermic peak at 369 °C characterizes the decomposition of the barb ligands. The decomposition ends at 467 °C to give presumably a mixture of sodium and silver oxides.

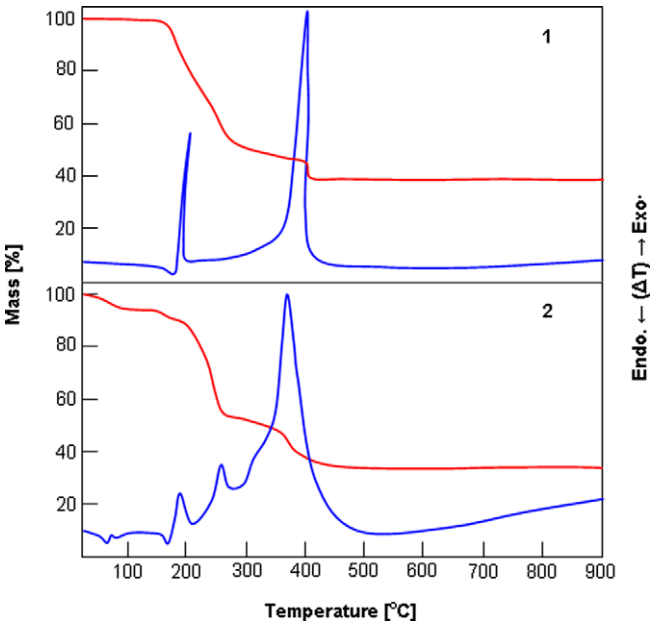

Fig. 3. DTA and TG curves of **1** and **2**.

4. Conclusions

In summary, two new coordination polymers, $[Ag_2(barb)(pipet)]_n$ (**1**) and $\{Na_3[Ag_2(barb)_2](pippr)\cdot 2H_2O\}_n$ (**2**) were synthesized and structurally characterized. Although in the metal complexes, 5,5-diethylbarbituric acid (H_2barb) usually exists in the Hbarb monoanion, the polymeric structures were achieved by the bridging of the barb dianion. In addition, a new coordination mode (tetradentate) of the barb dianion is observed.

Acknowledgements

We thank the research fund of Uludag University for the financial support given to the research project (F-2008/56).

Appendix A. Supplementary data

CCDC 748034 and 748035 contain the supplementary crystallographic data for **1** and **2**. These data can be obtained free of charge via http://www.ccdc.cam.ac.uk/conts/retrieving.html, or from the Cambridge Crystallographic Data Centre, 12 Union Road, Cambridge CB2 1EZ, UK; fax: (+44) 1223-336-033; or e-mail: deposit@ccdc.cam.ac.uk. Supplementary data associated with this article can be found, in the online version, at doi:10.1016/j.poly.2009.10.029.

References

[1] J.J.L. Zwicker, Pharm. Weekblad 68 (1931) 975.
[2] L. Levi, C.E. Hubley, Anal. Chem. 28 (1956) 1591.
[3] B.C. Wang, B.M. Craven, Chem. Commun. (1971) 290.
[4] L.R. Nassimbeni, A. Rodgers, Acta Crystallogr. B30 (1974) 2593.
[5] M.R. Caira, G.V. Fazakerley, P.W. Linder, L.R. Nassimbeni, Acta Crystallogr. B29 (1973) 2898.
[6] G.V. Fazakerley, P.W. Linder, L.R. Nassimbeni, A.L. Rodgers, Inorg. Chim. Acta 9 (1974) 193.
[7] L. Nassimbeni, A. Rodgers, Acta Crystallogr. B30 (1974) 1953.
[8] Y. Xiong, C. He, T.C. An, C.H. Cha, X.H. Zhu, Transition Met. Chem. 28 (2003) 69.
[9] K. Noguchi, H. Yuge, T.K. Miyamato, Acta Crystallogr. C56 (2000) e40.
[10] K. Noguchi, T. Tamura, H. Yuge, T.K. Miyamato, Acta Crystallogr. C56 (2000) 171.
[11] F. Yilmaz, V.T. Yilmaz, C. Kazak, Z. Anorg. Allg. Chem. 631 (2005) 1536.
[12] V.T. Yilmaz, F. Yilmaz, H. Karakaya, O. Buyukgungor, W.T.A. Harrison, Polyhedron 25 (2006) 2829.
[13] F. Yilmaz, V.T. Yilmaz, E. Bicer, O. Buyukgungor, Z. Naturforsch. 61b (2006) 275.
[14] F. Yilmaz, V.T. Yilmaz, E. Bicer, O. Buyukgungor, J. Coord. Chem. 60 (2007) 777.
[15] F. Yilmaz, V.T. Yilmaz, H. Karakaya, O. Buyukgungor, Z. Naturforsch. 63b (2008) 134.
[16] V.T. Yilmaz, M.S. Aksoy, O. Sahin, Inorg. Chim. Acta 362 (2009) 3703.
[17] M.S. Aksoy, V.T. Yilmaz, O. Buyukgungor, J. Coord. Chem. 62 (2009) 3250.
[18] V.T. Yilmaz, E. Soyer, E.O. Buyukgungor, J. Organomet. Chem. 694 (2009) 3306.
[19] G.M. Sheldrick, Acta Crystallogr. A64 (2008) 112.
[20] S. Hamamci, V.T. Yilmaz, O. Buyukgungor, J. Coord. Chem. Z. Naturforsch. 63b (2008) 139.
[21] B. Berking, B.M. Craven, Acta Crystallogr. B27 (1971) 1107.